Advanced Materials '93, I / B: Magnetic, Fullerene, Dielectric, Ferroelectric,
Diamond and Related Materials, edited by M. Homma et al.
Trans. Mat. Res. Soc. Jpn., Volume 14B

© 1994 Elsevier Science B.V. All rights reserved.

Recent progress in the development and analysis of coercivity of rare earth transition metal intermetallic compounds

H. Kronmüller

Institut für Physik, Max-Planck-Institut für Metallforschung,
Postfach 80 06 65, D-70506 Stuttgart 80, Germany

The coercive field of high-performance permanent magnets as produced by sintering, melt-spinning or mechanical alloying as a function of temperature in general can be described by a universal relation $H_c\ (T) = \alpha\ (T)\ H_N\ (T) - N_{eff}\ M_S$ where H_N denotes the ideal nucleation field and M_S the spontaneaous magnetization. The parameters α and N_{eff} describe the deteriorating effects of the microstucture. For approaching the optimal conditions $\alpha \rightarrow 1$ and $N_{eff} \rightarrow 0$ different types of procedures have to be combined: 1. Suitable additives (Nb, Mo, Al, Ga) for optimizing the microstructure. 2. Optimizing the grain size and sintering and annealing treatments. 3. Producing high-remanence magnets based as composite materials of nanocrystalline exchange coupled grains. The role of the parameters α and N_{eff} will be discussed on the basis of micromagnetism for individual grains and ensembles of grains.

1. INTRODUCTION

Rare-earth-transition-metal intermetallic compounds are the basis for high-quality permanent magnets with properties exceeding those of the hard-ferrites considerably [1-3]. Besides the Co-based compounds Co_5Sm and $Co_{17}Sm_2$ also the $Nd_2Fe_{14}B$ based magnets have become of importance. Furthermore, nitrides and carbides of type $Sm_2Fe_{17}N_{3-x}(C_{3-x})$ have become hopeful new materials. More recently, high-remanence composite magnets composed of nanocrystalline exchange coupled grains of a hard magnetic phase ($Sm_2Fe_{17}N_3$ or $Nd_2Fe_{14}B$) and a soft magnetic phase, e.g., α-Fe, have been propagated [4-6]. The application of all these alloys as permanent magnets (pms) is based on their intrinsic magnetic properties: High spontaneous magnetization, M_S, high anisotropy constants, K_i, high Curie temperatures. The characteristic properties of the hysteresis loops of high-quality pms should obey the following conditions:

1. Coercive field $\mu_0 H_c > 1.6$ T.
2. Remanent polarisation $\mu_0 M_R > 1.2$ T.
3. Energy product $(BH)_{max} > 200$ kJ/m³.
4. Rectangularity of the hysteresis loop.

The optimization and interpretation of these properties has been the subject of many papers [3,7].

2. MAGNETIC PROPERTIES AND THE MICROSTRUCTURE

During the last decade a large number of preparation techniques of pms have been developed leading to quite different microstructures concerning the grain sizes and the phase constitutions. In the case of an ideal pm ellipsoidal particles of the hard magnetic phase should be fully embedded in a non-magnetic phase being liquid during the sintering process, thus guaranteeing a high densification and an optimal magnetic decoupling of the individual grains. Actually, such an ideal

microstructure so far could not be realized. Nevertheless, an interpretation of the characteristic properties of the hysteresis loop in general starts from the results for the ideal system. In this case all properties are determined by the intrinsic material parameters (M_S, K_1). For real materials, however, the theoretical predictions have to be modified. This becomes evident if we consider the development of the ratio, H_c^{exp} / H_N, of the experimental coercive field to the ideal nucleation field, $H_N = 2K_1 / M_S$. As demonstrated in Fig. 1 the discrepancy between theory and experiment is of the order of a factor of 4. It is evident from this plot that the main progress comes from the development of new materials with large anisotropy constants, K_1, and suitable remanences, M_R.

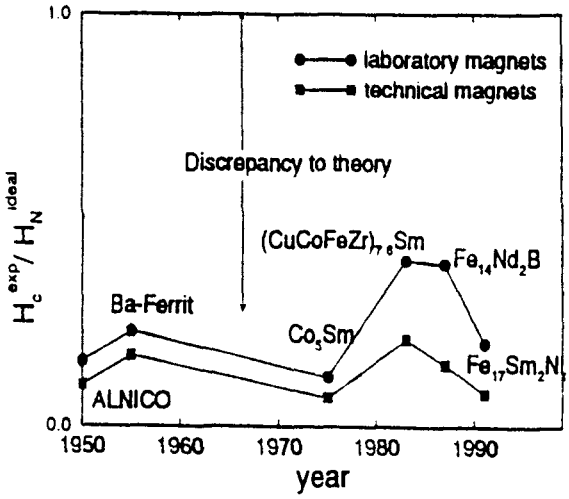

Figure 1. Ratio H_c^{exp} / H_N of prominent pms.

In order to explain the large gap between theory and experiment we have to take into account the role of the microstructures which may be quite different for pms produced by sintering, melt-spinning or mechanical alloying. Nevertheless, the characteristic properties of the hysteresis loops of pms are satisfactorily described by the following relations [7]:

$$H_c = (2K_1 / M_S)\,\alpha - N_{eff}\, M_S \qquad (1)$$

$$M_R = v\, M_S \,\langle \cos \psi \rangle \qquad (2)$$

$$(BH)_{max} = \frac{1}{4}\,\mu_0\, v^2\, M_S^2 \,\langle \cos^2 \psi \rangle \qquad (3)$$

The optimum energy product can only be achieved if the additional condition $\mu_0 H_c > \mu_0 M_R$ holds.

The microstructural parameter, α, describes the reduction of the ideal nucleation field due to reduced surface anisotropies and due to misaligned grains being coupled by dipolar long rang fields or by short range exchange interactions.

The effective demagnetization factor, N_{eff}, takes care of the short range dipolar fields at the edges and corners of polyhedral grains, and the angle, ψ, describes the misalignment of the grain's easy axes with respect to the alignment direction. A further parameter is the volume fraction, v, of the hard magnetic phase.

Eq. (1) has been applied successfully to a large number of magnetic materials produced by different techniques. A first approximation to take care of the microstructural effects is a factorization of α according to

$$\alpha = \alpha_K \cdot \alpha_\psi \ , \qquad (4)$$

where α_K describes the effects of the non-ideal particles - perturbation of the anisotropy constant at the grain surface or shape effects - whereas α_ψ takes care of the misalignment and the tpye of coupling between the grains. The parameter α_ψ has been determined for the case where also K_2 becomes important and is given by

$$\alpha_\psi = \frac{1}{\left(\cos^{2/3}\psi + \sin^{2/3}\psi\right)^{3/2}} \left\{ 1 + \frac{2K_2}{K_1} \frac{(tg\,\psi)^{2/3}}{1 + (tg\,\psi)^{2/3}} \right\} \qquad (5)$$

For $\psi = \pi/4$ we obtain $\alpha_{\pi/4} = 0.5 \cdot (1 + K_1/K_2)$.

The parameter α_K has been determined for planar perturbations of the anisotropy constant [7], and for a width $2r_0$ writes

$$\alpha_K = \delta_B / \pi r_0, \quad (2\pi r_0 \geq \delta_B) \qquad (6)$$

where $\delta'_B = \pi \sqrt{A/\Delta K_1}$ denotes a fictitious wall width in the region where K_1 is reduced by ΔK_1.

3. SOME EXPERIMENTAL RESULTS

3.1. Choice of additives

Extended magnetic and electron microscopy studies have shown that the characteristic properties of the hysteresis loops of $Nd_2Fe_{14}B$-based alloys may be sensitively influenced by small amounts of substitutional additives. These effects either are due to a change of the intrinsic magnetic material parameters or to a change of the microstructure. Three types of additives and their main effects are summarized in table 1. According to eq. (1) H_c may be increased either by increasing K_1 or by decreasing M_S. Dy is an element which fulfils both conditions simultaneously. However, concerning the energy product according to eq. (3) this seems to be a drawback. An alternative possiblility to increase H_c would be an optimization of the microstructural parameters with $\alpha \to 1$ and $N_{eff} \to 0$. In general large α-values are achieved by a suitable annealing treatment. Ga and Al have been found to enhance the magnetic decoupling between the grains by increasing the wettability of the liquid Nd-rich phase during the sintering process [8]. Ga in contrast to Al has the advantage not to dissolve in the $Nd_2Fe_{14}B$-grains appreciably, thus not reducing the spontaneous magnetization. Therefore, Ga combined with Nb or V, which inhibit grains growth, correspond to rather effective additives for achieving large coercive fields and large energy products.

3.2 Temperature dependence of H_c

The temperature dependence of H_c may be analysed by eq. (1) under the assumption that the temperature dependence of the parameter $\alpha = \alpha_K \cdot \alpha_\psi$ is predominantly determined by α_ψ (eq. (5)). In sect. 5 it will be shown that in the case of grains coupled by exchange or dipolar interactions always the grain with the largest misalignment determines H_c. In this case we choose for α_ψ its minimum values $\alpha_{45°}$. If the grains are magnetically isolated $\alpha_\psi^{int} = <\alpha_\psi>$ has to be used, where $<\alpha_\psi>$ denotes a volume average taking care of a Gaussian distribution function of the orientation of easy axes. The plot

Table 1
Role of additive elements in $Nd_2Fe_{14}B$

	Type I	Type II	Type III
Elements	Dy, Pr, Co, Al	Ga, Al, Cu	Nb, V, Mo
Constitutional Properties	Substitutionally dissolved in $Nd_2Fe_{14}B$ and in the intergranular phase	Increased viscosity of the intergranular liquid phase, small solubility in $Nd_2Fe_{14}B$	Formation of high-melting borides
Physical and metallurgical properties	Modification of intrinsic material parameters M_S, $K_{1,2}$, T_C	Magnetic decoupling of grains; improved corrosion	Inhibition of grain growth during sintering, improved corrosion

H_c^{exp} / M_S vs. $\left(2K_1 / M_S^2\right)\alpha_\psi^{eff}$ leads to a straight line with slope α_K and the intersection $(-)N_{eff}$ on the ordinate.

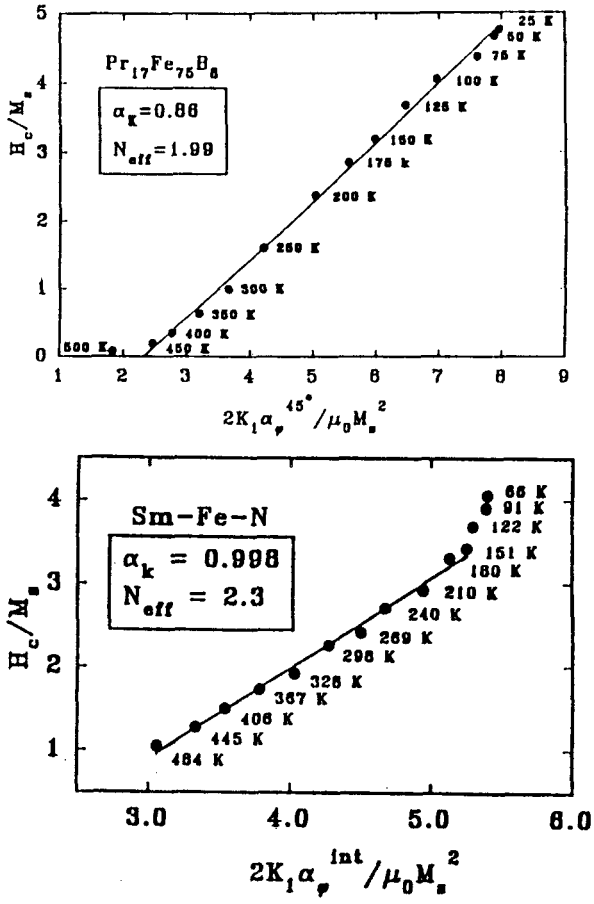

Figure 2. Analysis of the temperature dependence of $H_c(T)$. a) Sintered magnet $Pr_{17}Fe_{75}B_8$. b) Mechanically alloyed magnet $Sm_2Fe_{17}N_{3-x}$ [10].

Fig. 2a shows the plot of a sintered $Pr_{17}Fe_{75}B_8$ magnet giving for $\alpha_{45°}$ the values $\alpha_K = 0.86$, $N_{eff} = 1.99$. Fig. 2b gives the plot for a mechanically alloyed magnet $Sm_2Fe_{17}N_{3-x}$ where $<\alpha_\psi>$ has been used giving $\alpha_K = 0.998$ and $N_{eff} = 2.3$ [9].

4. DEMAGNETIZATION FIELDS IN REAL PARTICLES

In ellipsoidal particles the demagnetization field is homogeneous and of the order of $(-)1/3\ M_S$. If we deal with particles with sharp edges and corners, however, large demagnetization fields with logarithmic divergencies appear. Therefore, the arrangement of $\underline{M}_S$ near the edges becomes inhomogeneous leading to a remarkable reduction of the ideal nucleation field and also leading to a modification of the angular dependence of H_N.

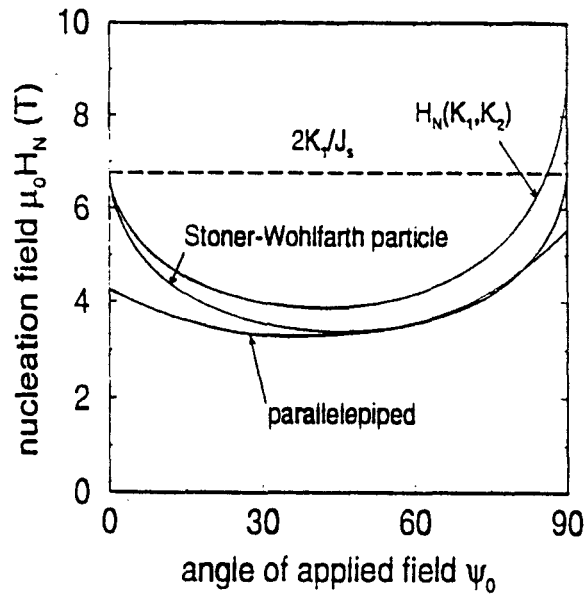

Figure 3. Angular dependence of the nucleation field for prisms of square cross-section (edge length 10 μm). Nucleation fields of the Stoner-Wohlfarth particle have been determined for K_1 as well as for K_1, K_2 and K_3.

Fig. 3 gives a comparison of the numerically determined angular dependence of H_c of an ellipsoidal $Nd_2Fe_{14}B$ particle with that of a prismatic particle of square cross-section [9]. The results of these calculations may be summarized as follows:

1. Also in polyhedral particles the reversion of M_S takes place at one unique nucleation field which, however, is significantly smaller than the ideal nucleation field.
2. The angular dependence of H_c is flattened as compared to the Stoner-Wohlfarth particle.
3. The temperature dependence of H_c follows eq. (1) with $\alpha_K = 0.94$, $\alpha_\psi = 1$ and $N_{eff} = 1.4$.

According to these results the effect of strong demagnetization fields at edges mainly contributes to the term $(-)N_{eff} M_S$.

5. ENSEMBLES OF MICROSCOPIC AND NANOCRYSTALLINE GRAINS

The micromagnetic results discussed so far are further modified if we consider ensembles of grains. In general neighbouring grains are coupled by short range exchange and/or dipolar long range interactions. Both types of interactions become important if within well oriented a misaligned grain exists. The results of a finite element computation are shown in fig. 4, where under the action of a reversed field $\underline{M}_S$ of a grain misaligned by 20° starts to rotate strongly and to initiate a cascade of spontaneous magnetization reversions within the neighbouring grains [11]. Fig. 4 shows demagnetization curves of four different types of couplings between the grains. The broken curve shows the result for the independent isolated grains obeying the Stoner-Wohlfarth theory. Curve A corresponds to exchange and dipolar coupled grains. Curve B shows the demagnetization curve for the partially dipolar and exchange coupled grains, and curve C corresponds to only dipolar coupled grains. It is obvious that in the latter three cases the demagnetization is determined exclusively by the misaligned grain and is more or less independent of the type of coupling between the grains.

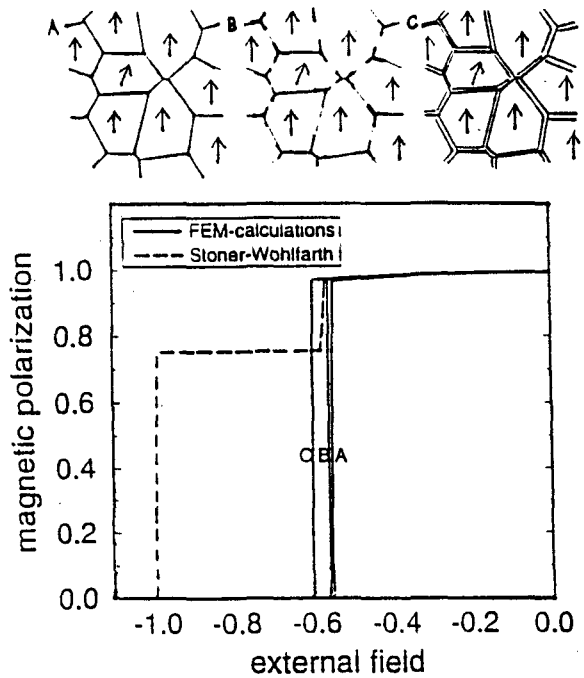

Figure 4. Demagnetization curves of an ensemble of grains with one grain misaligned by 20°. A) Exchange and dipolar interactions. B) Partial exchange and dipolar interactions. C) Only dipolar interactions. Isolated particles (---) [11].

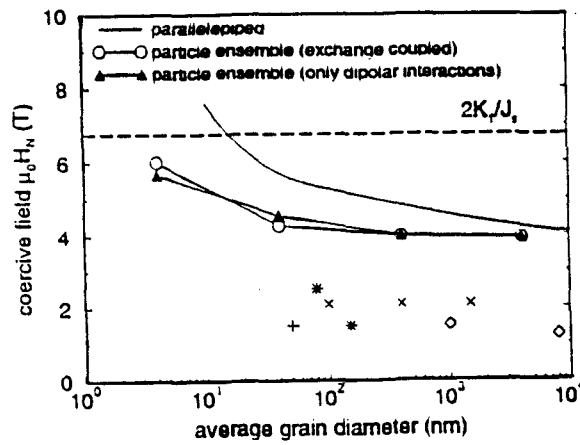

Figure 5. Nucleation fields of $Nd_2Fe_{14}B$ as a function of grain sizes. (—) prismatic particles with square cross-section. (-o-o-) exchange coupled ensembles. (-Δ-Δ-) dipolar coupled ensembles. (+, ×, *, ◊) experimental results [11].

There exists a moderate dependence of H_c on the grain size: The long range character of the stray fields decreases with decreasing grain size and due to the exchange coupling the misaligned grains become dominated by the well aligned grains if the grain size lies around or below the wall width, δ_B. This also is shown in fig. 5 where we present the grain size dependence of H_c for exchange and dipolar coupling and the free prismatic particles.

6. HIGH-REMANENCE COMPOSITE MAGNETS BY EXCHANGE HARDENING

In a number of papers [4-6] It has been proposed to produce high-remanence pms by using the exchange coupling between nanocrystalline magnetically hard and soft grains. Possible candidates for such pms are $Nd_2Fe_{14}B$, Co_5Sm, $Sm_2Fe_{17}N_{3-x}$ together with soft grains of α-Fe, Co or CoFe.

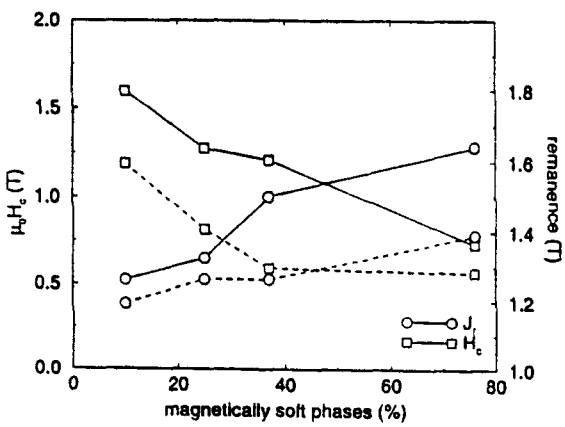

Figure 6. Remanence, coercivity and maximum energy product of composite magnets ($Nd_2Fe_{14}B$ + α-Fe) as a function of α-Fe content (full curves 10 nm, broken curves 20 nm).

For an isotropic ensemble of grains of the composite material $Nd_2Fe_{14}B$ + α-Fe by means of the finite element method H_c, M_R and $(BH)_{max}$ as a function of the amount of α-Fe have been determined for average grain diameters of 10 and 20 nm [12]. According to fig. 6 in the case of 40 % α-Fe the remanence, J_r, increases by 0.25 T whereas $\mu_0 H_c$ decreases by 0.30 T. Consequently, $(BH)_{max}$ increases by 50 % up to 450 kJ/m³ and the requirement $\mu_0 M_R < \mu_0 H_c$ still holds. For grains of diameters 20 nm the effects are less pronounced because the exchange effects have only an extension of the width of the domain wall.

REFERENCES

1. K.J. Strnat, J. Magn. Magn. Mat. 7 (1978) 351.
2. K.H.J. Buschow, Ferromagnetic Materials, Vol. 5, North-Holland Publ. Co., Amsterdam 1988, p. 1.
3. M. Sagawa and S. Hirosawa, J. Physique 49, C8 (1988) 617.
4. R. Coehorn, D.B. Mooji and C. de Waard, J. Magn. Magn. Mat. 80 (1989) 101.
5. J. Ding, Y. Liu, P.G. McCormick and R. Street, J. Magn. Magn. Mat. 123 (1993) L239; 124 (1993) 1.
6. R. Skomski and J. Coey, IEEE Trans. Magn., to be published.
7. H. Kronmüller, K.-D. Durst and M. Sagawa, J. Magn. Magn. Mat. 74 (1988) 291.
8. K.G. Knoch, Dr. rer. nat Thesis, University of Stuttgart, 1990.
9. H.F. Schmidts and H. Kronmüller, J. Magn. Magn. Mat., to be published.
10. X.C. Kou, W.J. Qiang, H. Kronmüller and L. Schultz, J. Appl. Phys., to be published.
11. T. Schrefl, H.F. Schmidts, J. Fidler and H. Kronmüller, J. Appl. Phys. 73 (1993) 6510.
12. T. Schrefl, J. Fidler and H. Kronmüller, J. Magn. Magn. Mat., to be published.